Received: 8 December 2022 | Accepted: 27 December 2022

DOI: 10.1111/ene.15669

european journal of neurology
the official journal of the european academy of neurology

ORIGINAL ARTICLE

Sporadic Creutzfeldt–Jakob disease is associated with reorganization of metabolic connectivity in a pathological brain network

Tomaž Rus[1,2] | Jernej Mlakar[3] | Luka Ležaić[4] | An Vo[5] | Nha Nguyen[6] | Chris Tang[5] | Michele Fiorini[7] | Elena Prieto[8] | Gloria Marti-Andres[9] | Javier Arbizu[8] | David Eidelberg[5] | Maja Trošt[1,2,4]

[1]Department of Neurology, University Medical Centre, Ljubljana, Slovenia

[2]Medical Faculty, University of Ljubljana, Ljubljana, Slovenia

[3]Institute of Pathology, Medical Faculty, University of Ljubljana, Ljubljana, Slovenia

[4]Department of Nuclear Medicine, University Medical Centre, Ljubljana, Slovenia

[5]Center for Neurosciences, Feinstein Institutes for Medical Research, Manhasset, New York City, USA

[6]Department of Genetics, Albert Einstein College of Medicine, Bronx, New York City, USA

[7]Section of Neuropathology, Department of Neuroscience, Biomedicine and Movement, University of Verona, Verona, Italy

[8]Department of Nuclear Medicine and Molecular Imaging, Clínica Universidad de Navarra, University of Navarra, Pamplona, Spain

[9]Department of Neurology, Clínica Universidad de Navarra, University of Navarra, Pamplona, Spain

Correspondence
Tomaž Rus, Department of Neurology, UMC Ljubljana, Zaloška 2, 1000 Ljubljana, Slovenia.
Email: tomaz.rus@kclj.si

Funding information
Fulbright Association; Javna Agencija za Raziskovalno Dejavnost RS

Abstract

Background and purpose: Although sporadic Creutzfeldt–Jakob disease (sCJD) is a rare cause of dementia, it is critical to understand its functional networks as the prion protein spread throughout the brain may share similar mechanisms with other more common neurodegenerative disorders. In this study, the metabolic brain network associated with sCJD was investigated and its internal network organization was explored.

Methods: We explored 2-[^{18}F]fluoro-2-deoxy-D-glucose positron emission tomography (FDG-PET) brain scans of 29 sCJD patients, 56 normal controls (NCs) and 46 other dementia patients from two independent centers. sCJD-related pattern (CJDRP) was identified in a cohort of 16 pathologically proven sCJD patients and 16 age-matched NCs using scaled subprofile modeling/principal component analysis and was prospectively validated in an independent cohort of 13 sCJD patients and 20 NCs. The pattern's specificity was tested on other dementia patients and its clinical relevance by clinical correlations. The pattern's internal organization was further studied using graph theory methods.

Results: The CJDRP was characterized by relative hypometabolism in the bilateral caudate, thalami, middle and superior frontal gyri, parietal lobe and posterior cingulum in association with relative hypermetabolism in the hippocampi, parahippocampal gyri and cerebellum. The pattern's expression significantly discriminated sCJD from NCs and other dementia patients ($p < 0.005$; receiver operating characteristic analysis CJD vs. NCs area under the curve [AUC] 0.90–0.96, sCJD vs. Alzheimer's disease AUC 0.78, sCJD vs. behavioral variant of frontotemporal dementia AUC 0.84). The pattern's expression significantly correlated with cognitive, functional decline and disease duration. The metabolic connectivity analysis revealed inefficient information transfer with specific network reorganization.

Conclusions: The CJDRP is a robust metabolic biomarker of sCJD. Due to its excellent clinical correlations it has the potential to monitor disease in emerging disease-modifying trials.

KEYWORDS
brain networks, Creutzfeldt–Jakob disease, Creutzfeldt–Jakob disease-related pattern, FDG-PET, graph theory

INTRODUCTION

Creutzfeldt–Jakob disease (CJD) is a fatal neurodegenerative rapidly progressing proteinopathy characterized by the deposition of misfolded prion protein [1]. Amongst the four etiology-related subtypes the sporadic form (sCJD) is the most common [2]. Although sCJD with an incidence of 1.4/million is a rare disease, it offers neuroscientists an in vivo model of neurodegeneration due to its short course, availability of pathological diagnosis and the relatively well-known mechanisms of prion protein propagation through the brain [3, 4]. sCJD is a uniformly fatal disease; however, new disease-modifying therapies are emerging [5] increasing the need for biomarkers to monitor disease.

The early diagnosis of sCJD may be challenging as its early presentation is diverse and may mimic other neurological, especially neurodegenerative, diseases [6]. The most common clinical presentation of sCJD is a rapidly progressing cognitive decline followed by extrapyramidal and cerebellar dysfunction, behavioral disturbances, myoclonus and akinetic mutism in the advanced stage [7]. A confirmation of prion protein in the brain is needed for a definite diagnosis, which is only possible at pathohistological examination [8]. Clinical diagnosis is based on typical presentation and rapid progression and is supported by the characteristic electroencephalography (EEG) changes, high levels of cerebrospinal fluid (CSF) protein 14-3-3 and/or typical magnetic resonance imaging (MRI) changes [9].

In contrast to extensive structural neuroimaging data, limited information is available about the characteristics and diagnostic utility of metabolic brain imaging. Case reports [10–13] and small case series [14–16] showed pronounced hypometabolism in various cortical and subcortical areas in CJD patients. The hypometabolic brain areas were concordant with MRI changes but more pronounced [16, 17]. To date, only three studies used a univariate voxel-vise statistical parametric mapping analysis of 2-[^{18}F]fluoro-2-deoxy-D-glucose (FDG) positron emission tomography (PET) scans to evaluate metabolic changes in sCJD [17–20].

Whilst univariate approaches analyze brain voxels independently of each other, multivariate analysis such as scaled subprofile model/principal component analysis (SSM/PCA) allows functionally connected areas in the brain tissue to be studied [21]. That said, multivariate approaches are particularly suitable in neurodegenerative disease research, where focal brain dysfunction affects the activity of various remote areas via neural networks [22]. Several researchers have used multivariate methods to identify abnormal metabolic brain networks in multiple neurodegenerative syndromes [22–25]. Furthermore, recent advances in graph theory methods have allowed us to study the internal organization of these networks (metabolic connectivity) in more detail [26, 27].

In this multicenter study, our aim was to identify and prospectively validate a multivariate sCJD-related pattern (CJDRP) by analyzing FDG-PET brain scans. To prove the pattern's specificity, its expression was tested on other dementia patients in comparison to sCJD. To explore its clinical relevance, patient's clinical features were correlated with the CJDRP expression. The CJDRP expression was also explored along different molecular subtypes of sCJD and its internal organization was studied using graph theory.

MATERIALS AND METHODS

Subjects

Identification cohort A

The CJDRP was identified in cohort A, which consisted of 16 pathologically confirmed sCJD patients and 16 age-matched normal control subjects (NCs) recruited from the University Medical Centre (UMC) Ljubljana, Slovenia. Patients underwent repeated EEG recordings, brain MRI and CSF analysis including 14-3-3 protein, tau, p-tau and amyloid-$\beta_{1\text{-}42}$. At autopsy, pathohistological, immunohistochemical and genetic analysis was performed. The demographic and clinical data of cohort A subjects are presented in Tables 1 and 2.

Cohort B

The pattern was prospectively validated in an independent cohort, which consisted of 13 sCJD patients and 20 NCs who underwent FDG-PET brain scan at the Clinica Universidad de Navarra, Spain. Nine patients had pathologically proven sCJD and the other four were diagnosed with probable sCJD [9]. Limited data of 10 patients had been presented previously [19].

Cohort C

To study the diagnostic specificity of CJDRP, FDG-PET brain scans of an additional 20 NCs, 26 Alzheimer's disease (AD) patients and 20 behavioral variant of frontotemporal dementia (bvFTD) patients from the UMC Ljubljana were analyzed. AD patients were clinically diagnosed with dementia, had Mini-Mental State Examination (MMSE) ≤25 and fulfilled the National Institute on Aging—Alzheimer's Association 2018 CSF criteria for AD [28]. The bvFTD group fulfilled diagnostic criteria of probable bvFTD [29].

TABLE 1 Demographic and clinical characteristics of pathologically confirmed sCJD patients from the identification cohort A

ID	Gender	Onset age	Survival (months)	First symptoms	Predominant symptoms	MMSE	CSF 14-3-3	CSF tau	Brain MRI[a]	EEG	PRNP 129 codon	PrP^{sc} type
1	M	50.9	6.3	Dysphagia, vertigo, balance problems	Cognitive decline	N/A	Positive	N/A	Positive	N/A	VV	2
2	F	63.9	1.8	Dysphasia, headache, cognitive decline	Aphasia, alien-limb syndrome, left-hand dystonia, cognitive decline	7/30	Positive	20,000	Positive	PSWC	MM	1
3	M	76.9	8.9	Parkinsonism, confusion	Parkinsonism, pyramid signs, myoclonus, cognitive decline	8/30	Negative	1739	Positive	PSWC	MM	2
4	F	76.4	8.0	Cognitive decline, hallucinations	Parkinsonism, pyramid signs, myoclonus, cognitive decline	7/30	Negative	3781	Positive	Progressive encephalopathy, periodic activity	MV	2
5	F	68.9	20.4	Ataxia, balance problems	Cognitive decline, hallucinations	21/30	Negative[b]	1868	Negative	Progressive encephalopathy, occasional periodic activity	MV	2
6	M	49.0	34.1	Cognitive decline	Cognitive decline, parkinsonism	14/30	Negative	857	N/A	Progressive encephalopathy, periodic arrhythmic theta activity	MV	2
7	F	58.1	5.2	Balance problems	Choreatic movements, hallucinations, cognitive decline	20/30	Positive	11,587	Positive	Progressive encephalopathy	VV	2
8	F	54.5	9.0	Acute psychosis	Ataxia, cognitive decline	10/30	Negative	1144	Positive	Non-specific changes	MV	1
9	M	79.1	2.9	Ataxia	Cognitive decline	21/30	Positive	11,599	Negative	Progressive encephalopathy	VV	2
10	M	63.5	2.2	Alien-limb syndrome	Ataxia, cognitive decline	27/28	Positive	13,345	Negative	PSWC	MM	2
11	M	77.4	1.3	Balance problems	Ataxia, cognitive decline, myoclonus	28/30	Positive	2365	Positive	PSWC	MM	1
12	M	65.4	1.6	Visual phenomena (hallucinations, Balint syndrome, micropsia)	Cognitive decline	6/27	Positive	11,164	Positive	PSWC	MM	1
13	M	67.4	1.9	Dysphasia, gait problems, cognitive decline	Ataxia, myoclonus, pyramid signs, cognitive decline	11/30	Positive	9605	Negative	PSWC	MM	1
14	F	85.5	2.7	Acute left-sided hemiparesis and hemihypaesthesia	Ataxia, myoclonus, alien-limb syndrome, cognitive decline	26/30	Positive	8434	Positive	PSWC	MM	1
15	F	79.7	6.6	Cognitive decline	Cortical blindness, hallucinations, myoclonus, decortical posture	9/30	Positive	3729	N/A	PSWC	MM	1
16	M	68.8	2.3	Ataxia	Myoclonus, cognitive decline	9/30	Positive	6482	Negative	Encephalopathy with slow activity	VV	2

Abbreviations: CSF, cerebrospinal fluid; MMSE, Mini-Mental State Examination; N/A, not available; PRNP, prion protein; PrP^{sc}, misfolded isoform of prion protein; PSWC, periodic sharp wave complexes.

[a]Positive/negative according to the diagnostic criteria.[9]

[b]Negative at the time of FDG-PET, later positive.

TABLE 2 Demographic and clinical characteristics of pathologically confirmed sCJD patients and NCs from the identification cohort A and its correlation with CJDRP expression. Characteristics that significantly differ between sCJD patients and NCs are emphasized in bold text.

		Normal controls ($N = 16$)	sCJD patients ($N = 16$)	p value[a]	Correlation with CJDRP expression
Demographic data	Age (years)	68.2 ± 4.9	68.1 ± 10.4	0.99	$R^2 = 0.03$, $p = 0.54$
Disease duration	Survival (months)		7.2 ± 8.4		$R^2 = 0.01$, $p = 0.69$
	Disease duration at FDG-PET (months)		4.7 ± 5.2		$R^2 = 0.03$, $p = 0.50$
	Relative disease duration at FDG-PET compared to survival		64.1% ± 16.3%		**$R^2 = 0.46$, $p = 0.004$**
Clinical scales	MMSE[c]	28.6 ± 1.2	15.0 ± 7.8	**<0.0001**	**$R^2 = 0.89$, $p < 0.0001$**
	MRC Prion Disease Rating Scale		10.6 ± 5.7		**$R^2 = 0.64$, $p = 0.0006$**
	CJD Neurological Status Scale		13.5 ± 8.2		**$R^2 = 0.49$, $p = 0.0025$**
CSF examination	tau		2172 ± 347		$R^2 = 0.02$, $p = 0.65$
	p-tau		63 ± 23		$R^2 < 0.01$, $p = 0.84$
	Amyloid-β		1078 ± 419		$R^2 < 0.01$, $p = 0.81$
sCJD subtype distribution	MM1/MV1		7 (44%)		$F_{3,12} = 0.8$, $p = 0.53$ (one-way ANOVA)[b]
	VV2		4 (25%)		
	MV2		3 (19%)		
	MM2		2 (12%)		
	VV1		0 (0%)		

Note: Mean values with standard deviations are presented.

Abbreviations: CSF, cerebrospinal fluid; CJDRP, sCJD-related pattern; FDG-PET, 2-[^{18}F]fluoro-2-deoxy-D-glucose positron emission tomography; MMSE, Mini-Mental State Examination; MRC, Medical Research Council; NCs, normal controls; sCJD, sporadic Creutzfeldt–Jakob disease.

[a]Comparison between NCs and sCJD using Student's t test.

[b]One-way ANOVA comparison of CJDRP z-scores amongst different subtypes of sCJD patients.

[c]The Mini-Mental State Examination (MMSE) was performed 3.7 ± 7.7 days before FDG-PET imaging.

FDG-PET image acquisition

Subjects from cohorts A and C underwent FDG-PET brain imaging at the Department of Nuclear Medicine at the UMC Ljubljana. They fasted a night before the procedure; after intravenous administration of FDG with 250 MBq activity, they rested in a quiet dark room with eyes closed for 30 min. Afterwards low dose attenuation correction CT and FDG-PET scan were performed using Siemens Biograph mCT PET/CT scanner. Images were reconstructed to 400×400 matrix with voxel size 1.02×1.02×3 mm and 4 mm Gaussian filter using the OSEM + PSF + TOF reconstruction algorithm.

Scanning of validation cohort B participants was conducted on a local imaging platform reported elsewhere [19]. The details of cohort B image reconstruction are presented in Supplementary material.

Image processing

FDG-PET scans were spatially normalized into a Montreal Neurological Institute (MNI) based PET template and smoothed using a three-dimensional Gaussian kernel using SPM5 software (Wellcome Trust Centre for Neuroimaging). A smoothing width of 10×10×10 mm full width at half maximum for cohorts A and C was used as described before [23]. Details of cohort B image preprocessing and harmonization are presented in Supplementary material.

Multivariate SSM-PCA for CJDRP identification

To identify and characterize a specific spatial covariance pattern associated with sCJD, FDG-PET scans of patients and NCs from cohort A were analyzed using an automatic voxel-based SSM/PCA procedure described elsewhere [21] (available at https://www.feinsteinneuroscience.org). After gray matter extraction with a custom mask based on the automated anatomical labeling atlas, automated principal component analysis was performed on a group of sCJD patients and NCs. Linearly independent covariance patterns (principal components, PCs) obtained in this way were linearly combined into a single spatial covariant CJDRP using the Akaike information criterion [23]. Expression of CJDRP (subject score) was computed in each subject's scan and was *z*-transformed with reference to the identification NC group (cohort A).

To overcome the impact of individual subjects and to determine the stability of the pattern, the bootstrapping procedure was performed using an in-house MATLAB script (1000 iterations) [30].

Validation of the CJDRP

The newly identified CJDRP was validated by four different approaches: (i) by the leave-one-out cross-validation (LOOCV) (detailed description in the Supplementary material) [31]; (ii) prospectively by studying the CJDRP expression in the independent cohort B of sCJD patients and NCs; (iii) by studying the CJDRP expression in cohort C (NCs, AD and bvFTD); (iv) by re-derivation of the CJDRP from cohort B and its comparison with the original pattern.

After LOOCV, single-subject CJDRP scores were prospectively calculated using the topographic profile rating algorithm in cohort B sCJD patients and NCs. Furthermore, to test the specificity of CJDRP, the expression scores were calculated also in cohort C in NCs, AD and bvFTD patients. All the expression scores were *z*-transformed according to the cohort A NCs. As the validation scans were obtained from two centers, the impact of different scanners and reconstruction algorithms were diminished by adjusting (offsetting) *z*-transformed values according to the average value of NCs from the corresponding center [32]. CJDRP expression scores were compared across the studied cohorts using one-way ANOVA and post hoc Bonferroni multiple comparison test.

The ability of the CJDRP to distinguish between sCJD and NCs in both cohort A (LOOCV subject scores) and cohort B as well as between sCJD and AD/bvFTD was studied by receiver operating characteristic (ROC) analysis by calculating the area under the curve (AUC).

Finally, to demonstrate CJDRP's repeatability, CJDRP was re-derived using NCs and CJD patients from cohort B as described above (called CJDRP-Spain). The similarity between the original CJDRP and CJDRP-Spain topographies was explored by voxel-wise Pearson correlational analysis incorporating a correction for spatial autocorrelation [33]. Thereafter, the CJDRP-Spain *z*-scores were calculated for NCs and CJD patients from cohorts A and B and correlated with the original CJDRP *z*-scores of the same patients (Pearson's correlation). To study differences in CJDRP-Spain *z*-scores amongst both NC and CJD groups one-way ANOVA was performed followed by the post hoc Bonferroni test.

Clinical correlations

To evaluate the clinical significance of the newly identified pattern, the correlations were studied between CJDRP expression and patients' clinical or laboratory measures: MMSE, Medical Research Council (MRC) Prion Disease Rating Scale [34], CJD Neurological Status Scale [35], CSF tau, p-tau and amyloid- β levels, age, survival (time span between first symptoms and death), disease duration at FDG-PET (time span between first symptoms and FDG-PET) and standardized disease duration (percentage of survival at FDG-PET = disease duration at FDG-PET/survival). Survival time, disease duration at FDG-PET and CSF tau were analyzed using nonparametric Spearman's correlation as these measures were not normally distributed. The remaining measures were analyzed by Pearson's correlation.

To further evaluate the prognostic value of CJDRP a Cox regression model was built using CJDRP adjusted for age, gender and CJD molecular subtype as independent variables and time to death as dependent variable.

Additionally, differences in CJDRP expressions were evaluated in different sCJD molecular subtypes (MM1/MV1, VV2, MV2, MM2 and VV1) using one-way ANOVA and post hoc Bonferroni comparison.

Internal network organization

Metabolic connectivity within the CJDRP vector space was studied using graph theory [26, 27, 36]. The CJDRP topographic map was transformed to regions of interest as described in Supplementary text and Table S1. Metabolic data from CJDRP-specific nodes were used to construct matrices of node-to-node pairwise correlations separately for CJD and NC subjects. In-house bootstrap methods were used to generate 100 samples for each group of subjects. The median value of 100 bootstrap correlation estimates for each correlation pair was used to create an adjacency matrix of each group graph.

To study the differences in global connectivity between CJD and NC networks in CJDRP space, the following network parameters were studied: degree centrality, random graph normalized clustering coefficient, random graph normalized characteristic path length, small-worldness and assortativity [26]. These measures were calculated for varying graph thresholds ranging from $r = 0.30$ to $r = 0.60$, at 0.05 increments, for all the 100 bootstrap iterations and compared between NCs and CJD using two-way repeated measures ANOVA.

The community structure of both CJD and NC networks was studied with Newman's modularity algorithm [37]. To better understand regional differences between CJD and NC networks in CJDRP space (i.e., connections gained and lost), all the connection pairs between NC and CJD networks were compared [26]. A detailed description of graph theory analysis is presented in the Supplementary material.

Statistical analysis

Logistic regression analysis was performed on JMP 14 software (SAS Institute Inc.). All other statistical tests were performed in GraphPad Prism 8 (GraphPad Software). For all comparisons, a p value below 0.05 was considered statistically significant. SPM12 (Institute of Neurology, UCL), BrainNet Viewer (National Key Laboratory of Cognitive Neuroscience and Learning, Beijing Normal University, Beijing, China) and MRIcro software (McCausland Center for Brain Imaging, University of South Carolina) were used for result visualization.

RESULTS

Subjects

Demographic and clinical data of the identification cohort A are presented in Tables 1 and 2. Age, gender and MMSE scores of all cohorts are presented in Table 3.

TABLE 3 Demographic data of subjects from all cohorts.

Cohort	*N*	Female/male	Age (mean ± SD)	MMSE (mean ± SD)
Cohort A				
NCs	16	10/6	68.2 ± 4.9	28.6 ± 1.2
sCJD	16	7/9	68.1 ± 10.7	15.0 ± 7.8
Cohort B				
NCs	20	8/12	68.1 ± 3.3	—
sCJD	13	4/9	66.0 ± 10.6	20.0 ± 6.9
Cohort C				
NCs	20	13/7	64.0 ± 7.7	29.0 ± 1.3
AD	26	14/12	74.3 ± 9.8	19.0 ± 4.9
bvFTD	20	13/7	68.8 ± 10.6	20.3 ± 4.9

Note: Number of patients (*N*), gender, age and Mini-Mental State Examination (MMSE) scores.

Abbreviations: AD, Alzheimer's disease; bvFTD, behavioral variant of frontotemporal dementia; NCs, normal controls; sCJD, sporadic Creutzfeldt–Jakob's disease; SD, standard deviation.

Sporadic CJD patients, bvFTD patients and NCs from different cohorts did not differ in age ($p > 0.99$). However, AD patients were on average older (significantly only compared to cohort C NCs; $p = 0.002$). Patients from different groups differed in MMSE (one-way ANOVA, $F_{5,105} = 22.7$, $p < 0.0001$): cohort A sCJD patients had lower MMSE compared to NCs, bvFTD and cohort B sCJD ($p < 0.05$), but not compared to the AD patients ($p = 0.06$).

Sporadic CJD-related pattern identification

The SSM-PCA resulted in a series of PCs amongst which a linear combination of PC1 and PC4 achieved the lowest Akaike information criterion and optimally discriminated between NCs and sCJD ($\chi^2 = 44.4$, $p < 0.0001$). The pattern was characterized by relative hypometabolism in the bilateral caudate, thalamus, frontal lobe (middle and superior frontal gyrus), parietal lobe (especially the precuneus) and middle and posterior cingulum. Relative hypermetabolism was observed in the bilateral hippocampus, parahippocampal gyri and a limited area of the anterior cerebellar lobe bilaterally and vermis (Figure 1a, Table S2). All regions were stable in the bootstrapping test at $p < 0.05$ ($z > 1.64$, one-tailed) (Figure S1). LOOCV showed significantly higher CJDRP z-scores in sCJD patients compared to NC subjects in the identification cohort A ($p = 8.8 \times 10^{-8}$, t test). The ROC analysis of the LOOCV CJDRP z-scores (CJD vs. NCs) resulted in AUC 0.96 (95% confidence interval [CI] 0.89–1.0, $p < 0.0001$).

Validations of CJDRP

In the validation cohort B, CJDRP expression scores prospectively computed in the sCJD patients were significantly higher than for the NC subjects (Figure 1b, right; $p < 0.0001$, t test corrected for

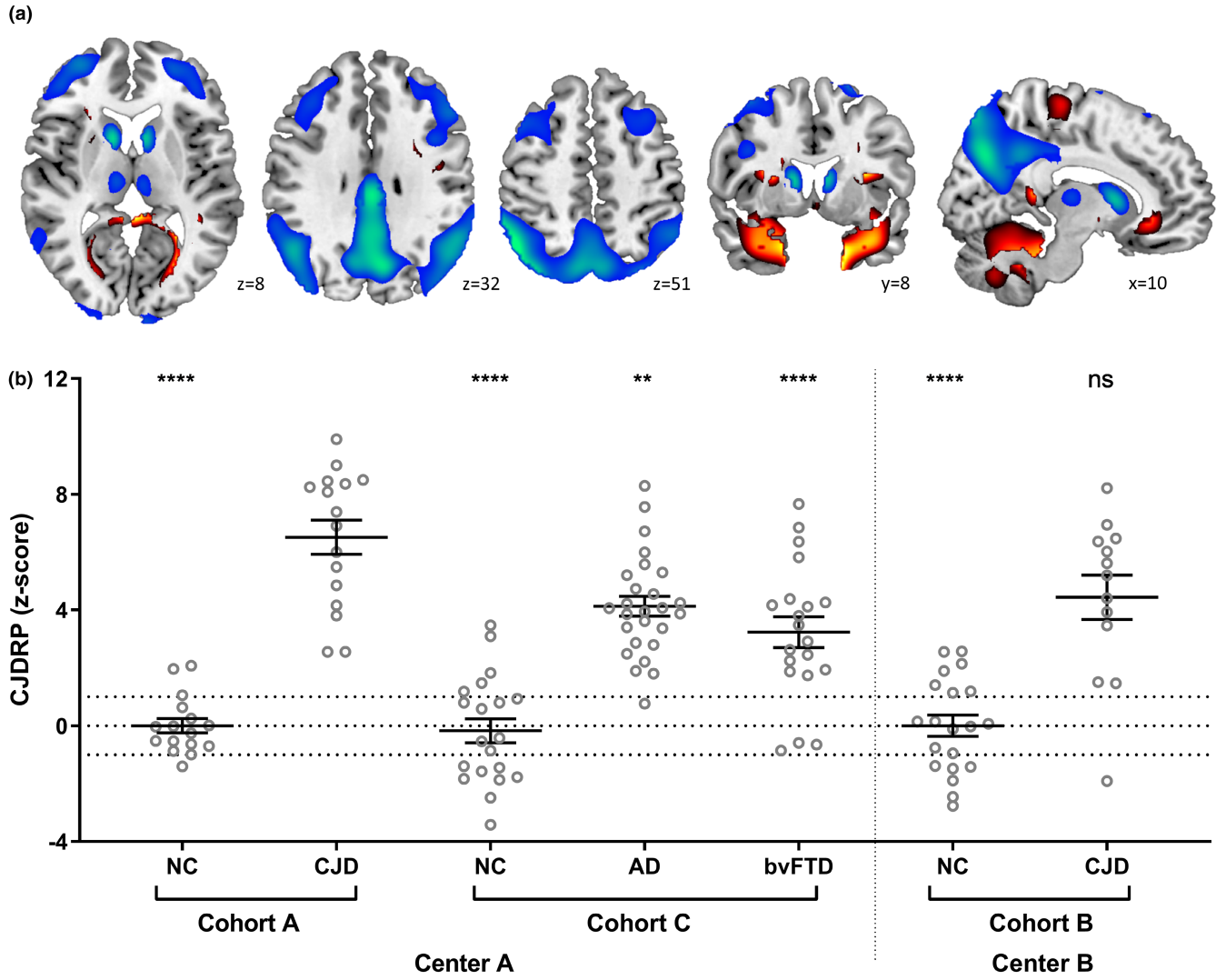

FIGURE 1 (a) Topography of the Creutzfeldt–Jakob disease-related pattern (CJDRP) and (b) CJDRP expression scores of subjects from the identification cohort A: normal controls (NCs) and Creutzfeldt–Jakob disease (CJD) patients; subjects from validation cohort C, NCs, Alzheimer's disease (AD) and behavior variant frontotemporal dementia (bvFTD) patients; and subjects from validation cohort B, NCs and CJD patients. (a) CJDRP was identified using multivariate SSM-PCA of FDG-PET images from 16 pathologically confirmed sCJD patients and 16 age-matched NCs. Relative metabolic decrease is color-coded blue and relative metabolic increase red. Coordinates in the axial (*z*), coronal (*y*) and sagittal (*x*) planes are in Montreal Neurological Institute standard space. (b) Mean values and standard errors are presented. A vertical line separates cohort B, which was adjusted (offset) according to the corresponding NCs. One-way ANOVA amongst all groups was performed ($F_{6,124} = 31.7$, $p < 0.0001$) and the results of a post hoc Bonferroni multiple comparison test between identification CJD group and other groups are presented. $^{**}p < 0.01$; $^{****}p < 0.0001$; ns, not significant $p > 0.05$.

multiple comparisons). No significant difference, however, was present between the two sCJD groups ($p = 0.13$) or between the two NC groups ($p = 0.99$) in the identification and validation cohorts A and C. Moreover, CJDRP scores differed significantly across the identification and validation cohorts of CJD, AD, bvFTD patients and NC subjects ($F_{6,124} = 31.7$, $p < 0.0001$) (Figure 1b, left); post hoc Bonferroni tests revealed significantly higher scores in CJD patients compared to AD, bvFTD and NC subjects ($p \leq 0.005$).

The discrimination ability of CJDRP to distinguish between CJD and NCs in the validation cohort B achieved AUC 0.90 (95% CI 0.76–1.0, $p < 0.0001$). ROC analysis of cohort A sCJD versus AD patients revealed an AUC of 0.78 (95% CI 0.63–0.94, $p = 0.002$) and versus bvFTD an AUC of 0.84 (95% CI 0.71–0.97, $p = 0.0006$).

In addition, to study the reproducibility of the pattern, an independent CJDRP-Spain was derived from NC and CJD subjects (cohort B). Both patterns exhibited remarkable similarity (Figure 2a): they significantly correlated voxel-wise ($r = 0.62$, $p < 0.001$) and on a single-subject basis ($r = 0.86$, $p < 0.0001$; Figure 2b,c). CJDRP-Spain *z*-scores significantly differed between CJD and NCs in both cohorts ($p < 0.0001$, post hoc Bonferroni test; Figure 2d).

Clinical correlation

An sCJD-related pattern expression correlated significantly with MMSE, MRC Prion Disease Rating Scale, CJD Neurological Status

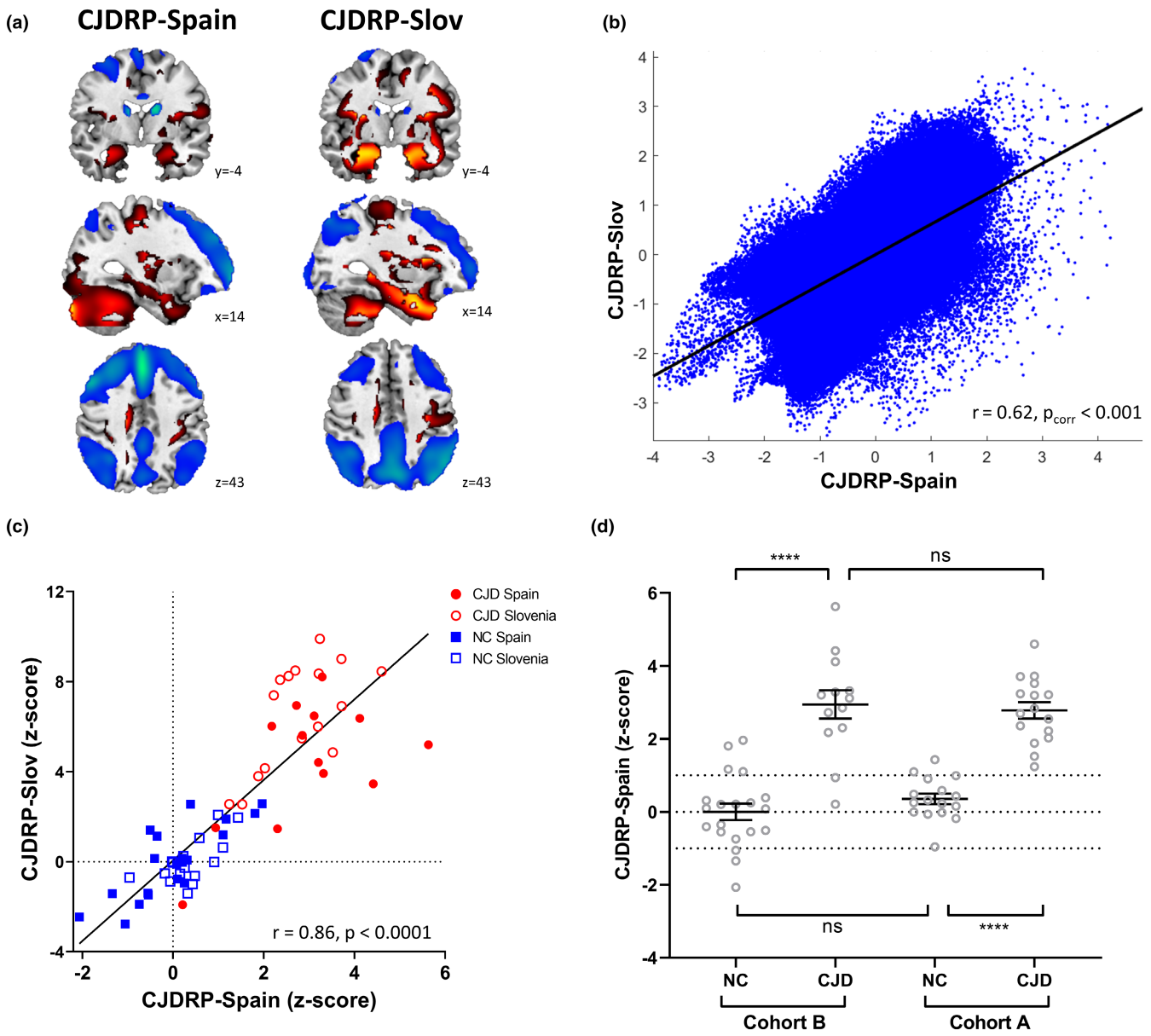

FIGURE 2 CJDRP-Spain derived from cohort B subjects in comparison with the original CJDRP (CJDRP-Slov). (a) Topographic representation of CJDRP-Spain (left) and the original CJDRP (CJDRP-Slov) (right). Relative hyperactive regions are color-coded red and relatively hypoactive regions color-coded blue. Coordinates in the axial (*z*), coronal (*y*) and sagittal (*x*) planes are in Montreal Neurological Institute standard space. (b), (c) Significant correlation was found between CJDRP-Spain and CJDRP-Slov topographies (b) ($r = 0.62$, $p < 0.001$, corrected for spatial autocorrelation) and between subject scores derived from both patterns (c) ($r = 0.86$, $p < 0.0001$). (d) CJDRP-Spain subject scores differed significantly between NCs and CJD patients from both cohorts, whilst no difference between NC or CJD groups was found (mean and standard error are presented; ns, not significant; ****$p < 0.0001$).

Scale and standardized disease (Figure 3a–d; $p \leq 0.004$) on FDG-PET imaging in cohort A. No correlations were found with subjects' age, survival time, absolute disease duration, CSF tau, p-tau or amyloid- β (Table 2).

The Cox regression model showed a significant effect of molecular subtype ($p = 0.001$, hazard ratios [HRs] of individual genotypes are presented in Table S3), age (HR 1.09 per year, 95% CI 1.01–1.21, $p = 0.01$) and CJDRP expression (HR 1.66 per unit, 95% CI 1.09–2.98, $p = 0.01$) on survival. Gender did not affect survival (HR 4.2 for male gender, CI 0.77–29.4, $p = 0.09$).

Sporadic CJD-related pattern *z*-scores did not differ between different sCJD molecular subtypes ($F_{3,12} = 0.8$, $p = 0.53$, post hoc Bonferroni comparison $p > 0.99$ for all the pairs).

Internal network organization

To better understand metabolic connectivity within CJDRP space, the differences in network organization between CJD patients and NCs were studied (Figure S2). All the studied parameters differed

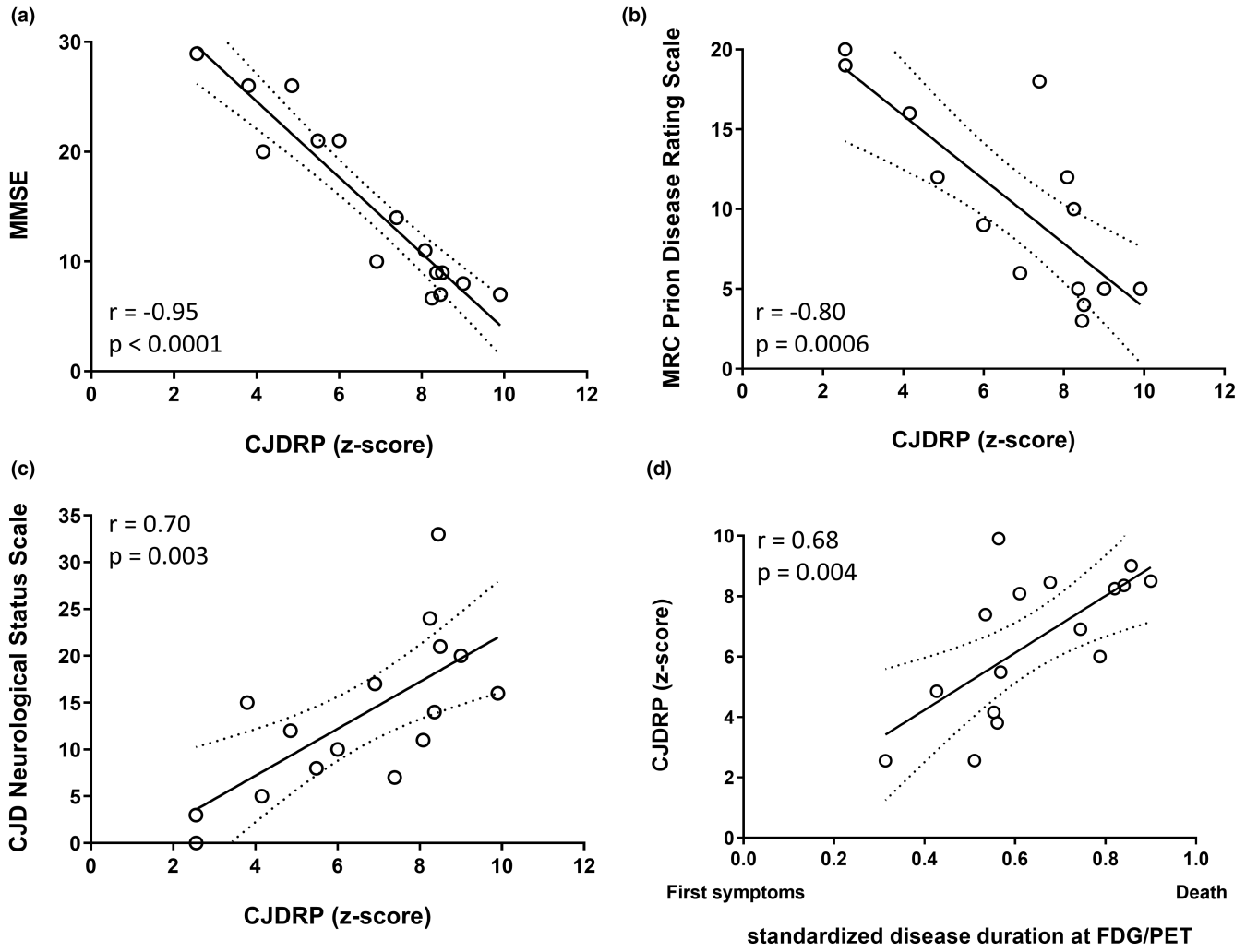

FIGURE 3 Correlations between CJDRP expression and clinical and demographic measures: (a) correlation with Mini-Mental State Examination (MMSE) score; (b) correlation with MRC Prion Disease Rating Scale;[34] (c) correlation with CJD Neurological Status Scale;[35] (d) correlation with standardized disease duration at FDG-PET (i.e., percentage of survival at FDG-PET).

significantly between CJD and NC networks. Whilst degree centrality was higher in CJD patients indicating an increased number of connections between nodes ($p < 0.0001$), the clustering coefficient indicating the network's local density was lower ($p = 0.04$). Characteristic path length, a measure of inefficiency of information transfer, was elevated ($p < 0.0001$) and the small-worldness coefficient, a measure combining the latter two, was lowered ($p < 0.0001$). Furthermore, assortativity, a graph theoretic measure indicating the tendency for network connections to link nodes with similar degree centrality, was highly elevated ($p < 0.0001$).

The NC and CJD graphs (Figure 4a,b) derived from median values of 100 bootstrap correlation estimates noticeably differed. In both NC and CJD networks two modules were found; however, they differed substantially (Table S1). In the CJD network, a significant loss of connections was found between the two modules (Figure 4c,d), predominantly between the parieto-occipital areas and the left hippocampus/temporal pole. Connections were predominantly gained within each module (Figure 4c,e). In addition, a gain of connection was noted also between modules: middle frontal gyri, left paracentral lobe and inferior parietal gyrus reconnected with temporal poles.

DISCUSSION

In the present study, the metabolic brain pattern specific for sCJD (CJDRP) was identified using a multivariate voxel-based spatial covariance analysis of the FDG-PET images in a homogeneous cohort of pathologically confirmed sCJD patients and validated with several methods. Its expression differed between different dementia syndromes but not across sCJD molecular subtypes. Its clinical relevance was proven by excellent correlations with several clinical measures. The graph theory analysis showed reorganization of the network with reduced efficiency of information transfer, disconnection between fronto-parieto-occipital and temporo-ventrolimbic modules, enhanced connectivity within local modules and novel reconnections between them.

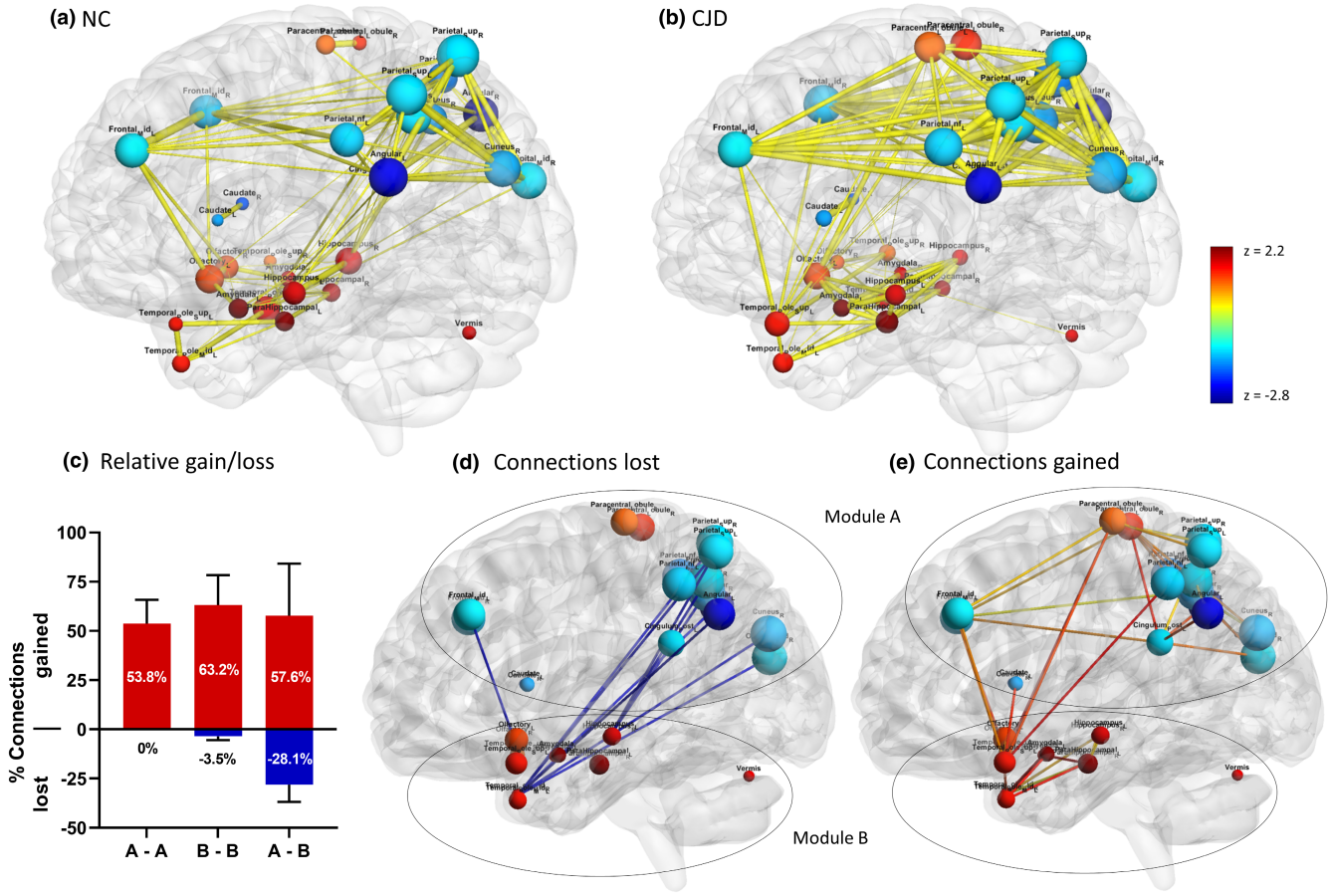

FIGURE 4 Metabolic connectivity within CJDRP space. Metabolic connectivity is presented for normal controls (NCs) (a) and Creutzfeldt–Jakob disease (CJD) patients (b). Reorganization of the network is evident. Two modules are indicated in both the NC and CJD graphs. Edge thickness corresponds to the magnitude of the correlation. All the edges exceeding $|r| > 0.6$ are presented. (c) Relative gain and loss of connections within module A (A–A), module B (B–B) and between the two modules (A–B). (Error bars represent median ± 95% confidence interval, 100 bootstrap iterations.) CJDRP community structure and connection gained (d) and lost (e) in the CJD network. Module A consisted of all the relatively hypoactive nodes and both paracentral nodes whilst module B consisted of all the remaining relatively hyperactive nodes. Significant functional connections gained or lost with respect to NCs are presented. Edge color corresponds to the magnitude of the correlation gained (yellow to red) or lost (blue). (Nodes are color-coded according to the CJDRP weights; the diameter of nodes corresponds to eigenvector centrality (see Section 2).

The CJDRP topography was largely consistent with previous smaller univariate studies [17–20]. Relative hypometabolism in the bilateral caudate, thalami and frontal areas have been described before by Prieto et al. [19], whilst Renard et al. [17, 20] and Kim et al. [18] described hypometabolism in frontal and parietal areas extending to the posterior cingulum. In all these studies, mesial temporal lobe metabolism was relatively preserved. In addition, the areas identified as metabolically hypoactive were most affected also in some studies investigating the distribution of characteristic MRI changes [38].

The validity of the newly identified CJDRP was proven by several independent methods, the stability of the pattern was proved by the bootstrapping test and the reproducibility by highly concordant pattern re-derivation on an independent group of CJD patients. CJDRP *z*-scores in sCJD patients were significantly higher compared to AD and bvFTD patients, proving a considerable specificity of the pattern in comparison to common neurodegenerative disorders with clinically overlapping presentation in early stages.

Whilst CJDRP expression scores differed amongst different dementia syndromes, this was not the case for molecular subtypes of sCJD. Namely, sCJD is a clinically and pathologically heterogeneous disease. The clinical phenotype, pathological findings as well as MRI changes are associated with six subtypes based on PRNP codon 129 polymorphism and protease resistence [39]. The most prevalent variant in the western hemisphere (and also in our sample; Table 2) is MM1/MV1 [40]. It is associated with pathological changes predominantly in the cerebral cortex, striatum, thalamus and somewhat less pronounced in the cerebellum with preserved hippocampus and brainstem nuclei [40]. CJDRP topography corresponds to the most affected regions observed in pathohistological studies in most of the subtypes [40]. However, the occipital cortex and cerebellum, where significant pathological changes are present in most prevalent variants, are spared in CJDRP topography. Interestingly, no difference in sCJD expression was found amongst different sCJD molecular subtypes. The effect of the genotype was insignificant

also after correction for standardized and absolute disease duration ($p = 0.52$ and $p = 0.59$, ANCOVA, analysis not shown). However, a small sample prevents us from drawing more precise conclusions. Nonetheless, these findings may indicate that advanced sCJD may not be as metabolically heterogeneous as may be assumed based on clinical, genetic and pathology case studies.

At this point, it should be stressed that the SSM-PCA method provides a network of covariate voxels and captures a network that is common to the whole group of included individuals regardless of their subtype. Several other neurodegenerative disorders may be subdivided into subtypes with different topographical metabolic profiles. Recent studies of multiple system atrophy [41] and progressive supranuclear palsy [42] have shown that the expression of a corresponding pattern is elevated in these patients regardless of disease subtype. As indicated by our results, the same may be true for sCJD. Alternatively, the CJDRP topography, despite being unique amongst neurodegenerative disorders, may be associated with advanced diffuse cerebral dysfunction rather than with the specific pathological process as more than half of cohort A CJD patients had advanced disease (Figure 3a,d). Interestingly, a topographically similar multivariate metabolic pattern was recently demonstrated in patients with coronavirus disease 19 (COVID-19) with neurological and cognitive symptoms [43]. Despite a different etiology and pathological process, similar networks may be involved in both diseases. Further studies exploring the relationship between histopathological and metabolic changes in CJD are under way. CJDRP expressions correlated with clinical scales and standardized disease duration, which denotes its clinical significance. The pattern had a very strong correlation with MMSE. Although the cognitive domains involved differ between different cognitive disorders [44], MMSE was found to be a good screening cognitive test irrespective of the nosological entity [45]. Notwithstanding, MMSE explores various cognitive domains that are characteristic for early prion disease (especially parietal dysfunction with impaired visuospatial performance, calculation and praxis, impairment of language and comprehension). Nevertheless, MMSE does not include executive function tests that were also shown to be affected early in prion diseases [46].

Whilst prior neuropsychological studies in sCJD patients revealed cognitive impairment in all cognitive domains, fronto-parietal domains were most affected with relative sparing of temporal lobe domains [46]. These findings are consistent with the pronounced fronto-parietal hypometabolism and relatively preserved temporal metabolism seen in CJDRP.

Furthermore, CJDRP expression strongly correlated with patients' functional measures and neurological status. A positive correlation with standardized disease duration provides an insight into the temporal progression of the neuropathological process, which seems to be fairly linear. A new measure of standardized disease duration was introduced due to the heterogeneous disease duration (41–1040 days). The survival in sCJD is known to be largely dependent on sCJD molecular subtype [40]. Indeed, the sCJD subtype was found to be a predicting variable of disease duration in FDG-PET and survival ($p = 0.008$ and $p = 0.02$; linear regression, analyses not shown) [47]. In addition to standardized disease duration, the prognostic value of CJDRP was demonstrated by conventional Cox regression analysis taking into account molecular subtype, age and gender.

The internal organization of the CJDRP network was studied using graph theory. At the global network level, the efficiency of information transfer, as shown by excessive characteristic path length and small-worldness coefficient, was reduced despite an increased number of overall connections as demonstrated by the exaggerated degree centrality in CJD compared to NCs. Increased degree centrality in severe neurodegenerative disorder may seem counterintuitive. However, further network exploration revealed inefficient reorganization as shown by exaggerated assortativity [27]. Indeed, the increase in degree centrality was primarily a result of a gain of new connections within the two modules whilst the loss of normal connections between the two modules contributed less. The disconnection between parieto-occipito-frontal and temporo-ventrolimbic areas may explain the severe cognitive decline despite preserved metabolism and relatively sparse histopathological findings in mesiotemporal lobes. Aberrant reconnection may represent an adaptive response of the network.

There are some noteworthy limitations of this study. First, although the current study is the largest analysis of brain metabolism in sCJD, the absolute number of subjects is still small due to the rarity of the disorder. Secondly, identification and validation scans were obtained from two different centers and, despite careful data harmonization, the acquisition and preprocessing parameters differ between centers. Further prospective validation of the pattern would certainly be welcome. Thirdly, whilst the CJDRP appears to be a disease-specific pattern amongst other neurodegenerative disorders, it is not known whether it is associated with the spread of a specific neuropathological process or a very advanced, less pathology-specific, brain network dysfunction.

In conclusion, metabolic CJDRP is a robust multivariate biomarker of sCJD that differentiates sCJD from NCs and other neurodegenerative dementia patients. It is replicable and appears to be independent of sCJD subtypes, the latter being a matter of ongoing research. This study provided an insight into the network-focused mechanisms of the disease demonstrating network disorganization and disconnection between vital network hubs. Due to its strong correlation with disease progression, CJDRP has a vast potential in emerging disease-modifying clinical trials [5]. This may have further vast applications as prion diseases are considered a model of neurodegeneration [3].

AUTHOR CONTRIBUTIONS

TR, DE, MT: Conception and design. TR, JM, LL, MF, ET, GMA, JA, MT: Acquiring data. TR, AV, NN, CT, DE: Analyzing data. TR: Drafting manuscript. CT, JA, DE, MT: Revising the manuscript. Approving the final content of the manuscript: all authors.

ACKNOWLEDGEMENTS

Professor Mara Popović is thanked for neuropathological consultation. Further, Assistant Professor Milica Gregorič Kramberger, Professor Zvezdan Pirtošek and other neurologists from the Department for Neurology, UMCL, are thanked for patients' referral.

FUNDING INFORMATION

Aspects of this work were supported by the Slovenian Research Agency through the research programme P1-0389, research project J7-2600. T.R. is a recipient of the Fulbright Foreign Student Program sponsored by the US Department of State's Bureau of Educational and Cultural Affairs.

CONFLICT OF INTEREST

The authors report no competing interests.

DATA AVAILABILITY STATEMENT

The data that support the findings of this study are available from the corresponding author, TR, upon reasonable request.

ETHICS STATEMENT

All procedures performed in the study involving human participants were in accordance with the ethical standards of the national research committee (the National Medical Ethics Committee of the Republic of Slovenia, 0120-584/2019/5) and with the 1964 Helsinki Declaration and its later amendments or comparable ethical standards.

ORCID

Tomaž Rus https://orcid.org/0000-0001-8019-0235

REFERENCES

1. Prusiner SB. Prions. *Proc Natl Acad Sci U S A*. 1998;95(23):13363-13383.
2. World Health Organisation. WHO manual for surveillance of human transmissible spongiform encephalopathies including variant Creutzfeldt–Jakob disease; 2003.
3. Jan A, Gonçalves NP, Vaegter CB, Jensen PH, Ferreira N. The prion-like spreading of alpha-synuclein in Parkinson's disease: update on models and hypotheses. *Int J Mol Sci*. 2021;22(15):8338. doi:10.3390/IJMS22158338
4. Duyckaerts C, Clavaguera F, Potier MC. The prion-like propagation hypothesis in Alzheimer's and Parkinson's disease. *Curr Opin Neurol*. 2019;32(2):266-271. doi:10.1097/WCO.0000000000000672
5. Mead S, Khalili-Shirazi A, Potter C, et al. Prion protein monoclonal antibody (PRN100) therapy for Creutzfeldt–Jakob disease: evaluation of a first-in-human treatment programme. *Lancet Neurol*. 2022;21(4):342-354. doi:10.1016/S1474-4422(22)00082-5
6. Rabinovici GD, Wang PN, Levin J, et al. First symptom in sporadic Creutzfeldt–Jakob disease. *Neurology*. 2006;66(2):286-287. doi:10.1212/01.wnl.0000196440.00297.67
7. Geschwind MD. Prion diseases. *Continuum*. 2015; 21(6 Neuroinfectious Disease):1612–1638. doi:10.1212/CON.0000000000000251
8. Budka H, Aguzzi A, Brown P, et al. Neuropathological diagnostic criteria for Creutzfeldt–Jakob disease (CJD) and other human spongiform encephalopathies (prion diseases). *Brain Pathol*. 1995;5(4):459-466. doi:10.1111/j.1750-3639.1995.tb00625.x
9. Zerr I, Kallenberg K, Summers DM, et al. Updated clinical diagnostic criteria for sporadic Creutzfeldt–Jakob disease. *Brain*. 2009;132(Pt 10):2659-2668. doi:10.1093/brain/awp191
10. Zizi G, Berger H, Lalire P, Dejust S, Morland D. ^{18}F-FDG PET/CT in sporadic Creutzfeldt–Jakob disease. *Clin Nucl Med*. 2020;45(7):538-539. doi:10.1097/RLU.0000000000003059
11. Obergassel J, Lohmann L, Meuth SG, Wiendl H, Grauer O, Nelke C. An enigmatic case of cortical anopsia: antemortem diagnosis of a 14-3-3 negative Heidenhain-variant MM1-sCJD. *Prion*. 2020;14(1):24-28. doi:10.1080/19336896.2019.1706703
12. Matías-Guiu JA, Guerrero-Márquez C, Cabrera-Martín MN, et al. Amyloid- and FDG-PET in sporadic Creutzfeldt–Jakob disease: correlation with pathological prion protein in neuropathology. *Prion*. 2017;11(3):205-213. doi:10.1080/19336896.2017.1314427
13. Morley NCD, Hofer M, Wilkinson P, Bradley KM. ^{18}FDG PET-CT in sporadic Creutzfeldt–Jakob disease, correlated with MRI and histology. *World J Nucl Med*. 2021;20(4):411-413. doi:10.4103/WJNM.WJNM_5_21
14. Na DL, Suh CK, Choi SH, et al. Diffusion-weighted magnetic resonance imaging in probable Creutzfeldt–Jakob disease: a clinical–anatomic correlation. *Arch Neurol*. 1999;56(8):951-957.
15. Engler H, Lundberg P, Ekbom K, et al. Multitracer study with positron emission tomography in Creutzfeldt–Jakob disease. *Eur J Nucl Med Mol Imaging*. 2003;30(1):85-95. doi:10.1007/s00259-002-1008-x
16. Xing XW, Zhang JT, Zhu F, et al. Comparison of diffusion-weighted MRI with ^{18}F-fluorodeoxyglucose-positron emission tomography/CT and electroencephalography in sporadic Creutzfeldt–Jakob disease. *J Clin Neurosci*. 2012;19(10):1354-1357. doi:10.1016/j.jocn.2011.11.035
17. Renard D, Vandenberghe R, Collombier L, Kotzki PO, Pouget JP, Boudousq V. Glucose metabolism in nine patients with probable sporadic Creutzfeldt–Jakob disease: FDG-PET study using SPM and individual patient analysis. *J Neurol*. 2013;260(12):3055-3064. doi:10.1007/s00415-013-7117-6
18. Kim EJ, Cho SS, Jeong BH, et al. Glucose metabolism in sporadic Creutzfeldt–Jakob disease: a statistical parametric mapping analysis of (18)F-FDG PET. *Eur J Neurol*. 2012;19(3):488-493. doi:10.1111/j.1468-1331.2011.03570.x
19. Prieto E, Domínguez-Prado I, Riverol M, et al. Metabolic patterns in prion diseases: an FDG PET voxel-based analysis. *Eur J Nucl Med Mol Imaging*. 2015;42(10):1522-1529. doi:10.1007/s00259-015-3090-x
20. Renard D, Castelnovo G, Collombier L, Thouvenot E, Boudousq V. FDG-PET in Creutzfeldt–Jakob disease: analysis of clinical–PET correlation. *Prion*. 2017;11(6):440-453. doi:10.1080/19336896.2017.1387348
21. Spetsieris PG, Ma Y, Dhawan V, Eidelberg D. Differential diagnosis of parkinsonian syndromes using PCA-based functional imaging features. *NeuroImage*. 2009;45(4):1241-1252. doi:10.1016/j.neuroimage.2008.12.063
22. Ma Y, Tang C, Spetsieris PG, Dhawan V, Eidelberg D. Abnormal metabolic network activity in Parkinson's disease: test–retest reproducibility. *J Cereb Blood Flow Metab*. 2007;27(3):597-605. doi:10.1038/sj.jcbfm.9600358
23. Tomše P, Jensterle L, Grmek M, et al. Abnormal metabolic brain network associated with Parkinson's disease: replication on a new European sample. *Neuroradiology*. 2017;59(5):507-515. doi:10.1007/s00234-017-1821-3
24. Meles SK, Pagani M, Arnaldi D, et al. The Alzheimer's disease metabolic brain pattern in mild cognitive impairment. *J Cereb Blood Flow Metab*. 2017;37(12):3643-3648. doi:10.1177/0271678X17732508

25. Nazem A, Tang CC, Spetsieris P, et al. A multivariate metabolic imaging marker for behavioral variant frontotemporal dementia. *Alzheimers Dement*. 2018;10:583-594. doi:10.1016/j.dadm.2018.07.009
26. Schindlbeck KA, Vo A, Nguyen N, et al. LRRK2 and GBA variants exert distinct influences on Parkinson's disease-specific metabolic networks. *Cereb Cortex*. 2020;30(5):2867-2878. doi:10.1093/cercor/bhz280
27. Vo A, Schindlbeck KA, Nguyen N, Rommal A, Spetsieris PG, Tang CC, Choi YY, Niethammer M, Dhawan V, Eidelberg D Adaptive and pathological connectivity responses in Parkinson's disease brain networks. *Cereb Cortex* Published Online March 25, 2022;33(4):917–932. doi:10.1093/CERCOR/BHAC110
28. Jack CR, Bennett DA, Blennow K, et al. NIA-AA research framework: toward a biological definition of Alzheimer's disease. *Alzheimers Dement*. 2018;14(4):535-562. doi:10.1016/j.jalz.2018.02.018
29. Rascovsky K, Hodges JR, Knopman D, et al. Sensitivity of revised diagnostic criteria for the behavioural variant of frontotemporal dementia. *Brain*. 2011;134(9):2456-2477. doi:10.1093/BRAIN/AWR179
30. Bradley E, Robert T. *An Introduction to the Bootstrap*. Chapman & Hall; 1994.
31. Teune LK, Renken RJ, Mudali D, et al. Validation of parkinsonian disease-related metabolic brain patterns. *Mov Disord*. 2013;28(4):547-551. doi:10.1002/mds.25361
32. Tomše P, Peng S, Pirtošek Z, et al. The effects of image reconstruction algorithms on topographic characteristics, diagnostic performance and clinical correlation of metabolic brain networks in Parkinson's disease. *Phys Med*. 2018;52:104-112. doi:10.1016/j.ejmp.2018.06.637
33. Ko JH, Spetsieris P, Ma Y, Dhawan V, Eidelberg D. Quantifying significance of topographical similarities of disease-related brain metabolic patterns 2014; 9(1):e88119.
34. Thompson AGB, Lowe J, Fox Z, et al. The Medical Research Council prion disease rating scale: a new outcome measure for prion disease therapeutic trials developed and validated using systematic observational studies. *Brain*. 2013;136(4):1116-1127. doi:10.1093/brain/awt048
35. Cohen OS, Prohovnik I, Korczyn AD, et al. The Creutzfeldt–Jakob disease (CJD) neurological status scale: a new tool for evaluation of disease severity and progression. *Acta Neurol Scand*. 2011;124(6):368-374. doi:10.1111/j.1600-0404.2011.01489.x
36. Ko JH, Spetsieris PG, Eidelberg D. Network structure and function in Parkinson's disease. *Cereb Cortex*. 2018;28(12):4121-4135. doi:10.1093/CERCOR/BHX267
37. Newman MEJ. Modularity and community structure in networks. *Proc Natl Acad Sci*. 2006;103(23):8577-8582. doi:10.1073/PNAS.0601602103
38. Tschampa HJ, Kallenberg K, Kretzschmar HA, et al. Pattern of cortical changes in sporadic Creutzfeldt–Jakob disease. *Am J Neuroradiol*. 2007;28(6):1114-1118. doi:10.3174/AJNR.A0496
39. Hermann P, Appleby B, Brandel JP, et al. Biomarkers and diagnostic guidelines for sporadic Creutzfeldt–Jakob disease. *Lancet Neurol*. 2021;20(3):235-246. doi:10.1016/S1474-4422(20)30477-4
40. Parchi P, Giese A, Capellari S, et al. Classification of sporadic Creutzfeldt–Jakob disease based on molecular and phenotypic analysis of 300 subjects. *Ann Neurol*. 1999;46(2):224-233. doi:10.1002/1531-8249(199908)46:2<224::AID-ANA12>3.0.CO;2-W
41. Tomše P, Rebec E, Studen A, et al. Abnormal metabolic covariance patterns associated with multiple system atrophy and progressive supranuclear palsy. *Phys Med*. 2022;98:131-138. doi:10.1016/J.EJMP.2022.04.016
42. Martí-Andrés G, van Bommel L, Meles SK, et al. Multicenter validation of metabolic abnormalities related to PSP according to the MDS-PSP criteria. *Mov Disord*. 2020;35(11):2009-2018. doi:10.1002/MDS.28217
43. Hosp JA, Dressing A, Blazhenets G, et al. Cognitive impairment and altered cerebral glucose metabolism in the subacute stage of COVID-19. *Brain*. 2021;144(4):1263-1276. doi:10.1093/BRAIN/AWAB009
44. Ridha B, Rossor M. The Mini Mental State Examination: how to do it. *Pract Neurol*. 2005;5(5):298-303.
45. Tombaugh TN, McIntyre NJ. The Mini-Mental State Examination: a comprehensive review. *J Am Geriatr Soc*. 1992;40(9):922-935. doi:10.1111/j.1532-5415.1992.tb01992.x
46. Caine D, Tinelli RJ, Hyare H, et al. The cognitive profile of prion disease: a prospective clinical and imaging study. *Ann Clin Transl Neurol*. 2015;2(5):548-558. doi:10.1002/acn3.195
47. Krasnianski A, Schulz-Schaeffer WJ, Kallenberg K, et al. Clinical findings and diagnostic tests in the MV2 subtype of sporadic CJD. *Brain*. 2006;129(9):2288-2296. doi:10.1093/brain/awl123

SUPPORTING INFORMATION

Additional supporting information can be found online in the Supporting Information section at the end of this article.

How to cite this article: Rus T, Mlakar J, Ležaić L, et al. Sporadic Creutzfeldt–Jakob disease is associated with reorganization of metabolic connectivity in a pathological brain network. *Eur J Neurol*. 2023;30:1035-1047. doi:10.1111/ene.15669